IJE TRANSACTIONS B: Applications Vol. 26, No. 5, (May 2013) 473-488

International Journal of Engineering

Journal Homepage: www.ije.ir

Aqueous Cadmium Ions Removal by Adsorption on APTMS Grafted Mesoporous Silica MCM-41 in Batch and Fixed Bed Column Processes

F. Ghorbani[a], H. Younesi*[a], Z. Mehraban[b], M. Sabri Celik[c], A. A. Ghoreyshi[d], M. Anbia[e]

[a] *Department of Environmental Science, Faculty of Natural Resources, Tarbiat Modares University, 64414-356 Noor, Iran.*
[b] *New Technologies Committee, Research Institution for Curriculum Development and Educational Innovations, 1584634818, Tehran, Iran.*
[c] *Mining Engineering Department, Mineral and Coal Processing Section, Istanbul Technical University, Ayazaga, 80626 Istanbul, Turkey.*
[d] *Biotechnology Research Lab., Faculty of Chemical Engineering, Noshirvani University, Babol, Iran.*
[e] *Research Laboratory of Nanoporous Materials, Faculty of Chemistry, Iran University of Science and Technology, Farjam Street, Narmak, 16846, Tehran Iran.*

PAPER INFO

Paper history:
Received 23 November 2012
Recivede in revised form 11 December 2012
Accepted 13 December 2012

Keywords:
Sedge (*Carex riparia*)
MCM-41
Batch Adsorption
Fixed-bed Column

ABSTRACT

Highly ordered mesoporous MCM-41silica with hexagonal structure was synthesized using extracted amorphous silica from sedge (*Carex riparia*) ash. Obtained mesoporous materials functionalized by 3-(Aminopropyl) trimethoxysilane (APTMS) and their structures characterized by means of X-ray diffraction (XRD), nitrogen adsorption-desorption, thermogravimetric analysis (TGA) and Fourier transform infrared (FT-IR) spectroscopy. The synthesized material were applied for adsorption of Cd(II) metal ions from aqueous solution in batch and fixed bed column systems. Batch adsorption process was carried out to evaluate initial ion concentrations, sorbent dose, contact time, pH and temperature. The equilibrium data were analyzed using the Langmuir and Freundlich isotherm by nonlinear regression analysis. The kinetics study reviled that data from the experiments fitted well to the pseudo-second order equation than pseudo-first order. Thermodynamic parameters reviled that the adsorption process strongly depended on temperature and the adsorption capacity increased by increasing the temperature of the system, indicating the endothermic behavior and spontaneous nature of adsorption. For continuous adsorption experiments, NH_2-MCM-41 adsorbent was used and breakthrough curves were analyzed at different bed heights, flow rates and initial metal ion concentrations. Thomas and bed depth service time (BDST) models were used to determine the kinetic constants and to predict the breakthrough curves of each component.

doi: *10.5829/idosi.ije.2013.26.05b.03*

1. INTRODUCTION

The contamination of water by toxic heavy metals is a worldwide environmental problem. Heavy metals, particularly cadmium, can not only have toxic and harmful effects on organisms living in water, but also accumulate throughout the food chain and may also affect human beings [1]. Cadmium pollutant is found in wastewaters from chemical manufacturing, painting, coating, and greatly threaten the health of human populations and the natural ecosystems [2]. The harmful effects of cadmium reported include a number of acute and chronic disorders, such as itai-itai disease, renal damage, emphysema, hypertension and testicular atrophy. It has been consistently desired that heavy metals level be reduced in industrial and municipal effluents before ultimate repository in the ecosystem. Different developed methods that could be used to remove dissolved heavy metal ions from wastewaters include chemical precipitation, chemical oxidation and reduction, ion exchange, filtration, electrochemical treatment, membrane technologies, adsorption and evaporative recovery [3]. Ion exchange and adsorption are the most common and effective processes for this purpose [4]. Many adsorption studies have been done to remove Cd(II) from aqueous solutions by utilizing functionalized materials with several different types of substrates, such as polymers [5], zeolites [6], clays [7] and activated carbon [8]. Nevertheless, some materials suffer from inherent problems, such as low removal capacity, low selectivity, long equilibrium time,

*Corresponding Author Email: hunesi@modares.ac.ir, hunesi@yahoo.com (H. Younesi)

mechanical and thermal instability [9]. Recently, mesoporous materials have been paid special attention owing to their scientific importance and great potentials in practical applications such as catalysis [10], adsorbents [11, 12] and sensors. Ordered mesoporous silica are materials that not only have a large surface area and pore volume but also high physico-chemical stability, high thermal stability, uniform pore size distribution, long-range homogeneity of texture and ease of surface modifications [13, 14], thus having great potential as adsorbents. Within this group, MCM-41 is typical and characterized by parallel and ideally shaped pore structures without the complications of a network. The cylindrical pore structure and high degree of pore symmetry found in MCM-41 have made it an ideal candidate for testing various existing adsorption and diffusion models [15]. The surface of the MCM-41 can be improved by functionalization to make it an ideal organic/inorganic hybrid adsorbent. However, both the economic and environmental costs for the large-scale manufacture of mesoporous silica compounds are high, owing to the cost and toxicities of both the templates and the variety of silica sources including sodium silicate, fumed silica and silicon tetraethoxide [16]. Recently, the use of the waste products like rice husk and fly ash from rice milling and coal combustion, which contains around 95% silica, have been proved to be potential silica sources for the synthesis of mesoporous silica [17, 18].

In the present study, sedge (*Carex riparia*) ash was used as a new silica source [19] to synthesize mesoporous MCM-41and grafting its defective Si–OH groups with 3-aminopropyl trimethoxysilane (APTMS). MCM-41 and NH_2-MCM-41 were used to remove Cd(II) metal ions from aqueous solution in batch and fixed bed column systems. The effects on the adsorption behavior of the removal process parameters such as adsorbent dose, solution pH, metal ions concentration, and temperature were studied. Well-known isotherm and kinetic models were applied to analyze the equilibrium data and thermodynamic parameters (enthalpy, entropy and adsorption free energy), which were then also calculated to describe the adsorption mechanism. Further, the investigation was conducted to remove Cd(II) ions from aqueous solution by NH_2-MCM-41 as adsorbent in the fixed bed column. In addition, to examine the effects of operational conditions such as bed height, flow rate and metal ion concentration on the column dynamics. The dynamics of the adsorption process was analyzed by application of Thomas and BDST models.

2. MATERIAL AND METHODS

2. 1. Chemicals Acetic acid, hexadecyltrimethylammoniumbromide (CTAB), 3-aminopropyl trimethoxysilane (APTMS), n-hexane, hydrochloric acid (37%), sodium hydroxide (NaOH) were all purchased from Aldrich and used with no further purification. $CdSO_4$. 8/3 H_2O powder were purchased from Merck (Darmstadt, Germany) and used for Cd(II) stock solution preparation. All reagents were used in their analytical grade without further purification. Deionized distilled water was used to prepare all solutions.

2. 2. Synthesis of MCM-41 Mesoporous Silica The mesoporous MCM-41 was prepared as reported elsewhere [19]. Briefly, SiO_2 (98%) powder that extracted from sedge (11 g) was predispersed in deionized water (175 ml) containing NaOH (6.25 g) with stirring. Then, the whole system was introduced in an oil bath and refluxed at 80 ^oC for 24 h. An aqueous solution of hexadecyltrimethylammoniumbromide (CTAB) prepared separately by mixing CTAB (3.75 g) and deionized water (62.5 ml). Surfactant solution was slowly added to the sodium silicate solution under stirring. After adjusting the pH to 11 using 5N acetic acid, the mixture was stirred vigorously at room temperature for 6 h. The surfactant-silica gel mixture was heated at 100˚ C for 72 h in polypropylene bottle. Yet again, the pH was adjusted to 11 using acetic acid and aged for 24 h. Finally, the solid product was filtrated, washed with DI water, and dried at 80˚ C overnight. Removal of the template was performed by soxhlet extraction in acidic ethanol (20 ml ethanol and 0.5 ml HCl per 1 g MCM-41) for 72 h and either by calcinations in air at 550 ^oC for 5 h to completely remove the surfactant template.

2. 3. Synthesis of NH_2–MCM-41 The amine functionalized MCM-41 was prepared according to the method described in the literature [14]. Exactly, 30 mmol APTMS was added drop wise to 5 g of vacuum dried mesoporous silica MCM-41 dispersed in 250 ml of n-hexane under vigorous stirring and N_2 atmosphere. Then the mixture was refluxed at 80 ^oC for 24 h and the final product was filtered, washed several times with n-hexane and dried in desiccators for 24 h. The products were represented as NH_2–MCM-41.

2. 4. Characterization The crystalline structure of produced silica and synthesized MCM-41 were examined by X-ray diffraction of samples recorded with a GBC-Difftech MMA diffractometer. The nickel filtered Cu Kα (λ= 1.54A˚) radiation was used at acceleration voltage of 35 kV and current of 34.2 mA. The diffraction angle was scanned from 1˚ to 10˚, 2θ, at a rate of 1˚/min. Fourier transform infrared spectroscopy (FTIR) experiment was carried out by FTIR1650 spectrophotometer (Shimadzo, Japan) in the range of 400–4000cm^{-1} employing the KBr pellet method (sample/KBr= 1/100). In order to determine the textural

properties, the nitrogen adsorption-desorption isotherms were measured using a BEL sorp-mini II volumetric adsorption analyzer in order to determine the textural properties. All of the samples were degassed at 100◦C under an argon gas flow for 3 h before analysis. The concentrations of residual Cd(II) ions in the supernatant solutions were determined using flame atomic absorption spectrophotometer (Philips, PU9400, USA).

2. 5. Batch Adsorption Procedure and Modeling Batch adsorption experiments were conducted to evaluate the MCM-41 and NH_2-MCM-41 capacities. Each experiment was carried out in 250 ml Erlenmeyer flasks containing 100 ml Cd(II) solution by shaking the flasks at 120 rpm for period contact time of 120 min. Samples were withdrawn at predetermined time intervals (0, 5, 15, 30, 60, 90 and 120 minutes) and filtered through 0.25μm filters. Filtered samples were analyzed for residual Cd(II) ion concentration. The effects of the dose of MCM-41(0.5, 1, 1.5 and 2 gl^{-1}) and NH_2-MCM-41(0.1, 0.5, 1, 1.5, 2, 2.5, 3 and 3.5 gl^{-1}) adsorbents on adsorption of Cd(II) metal ions at 100 mgl^{-1} were studied. The pH of the working solutions was adjusted to 5. To examine the effect of pH, adsorption experiments were conducted at different pH ranging from 2 to 8 at 100 mg l^{-1} of Cd(II) solution. For kinetic studies deferent initial concentrations of Cd(II) solutions including 10, 25, 50, 100, 150 and 200 mgl^{-1} were chosen. The adsorption process was evaluated at constant temperatures of 20, 30, 40 and 50 °C respectively, for the adsorption isotherms as well as the thermodynamic studies.

The removal efficiency of the metal ions was calculated by the following equation (Equation 1):

$$R = \frac{C_i - C_t}{C_t} \times 100 \quad (1)$$

Where R is the removal efficiency of the metal ions, C_i and C_t are the initial concentration and concentration of the metal ions in $mg.l^{-1}$ at t time, respectively.

Metal uptake was determined according to Equation (2):

$$q_e = \frac{V(C_i - C_e)}{S} \quad (2)$$

Where q_e is the amount of metal ions adsorbed on the sorbent in $mg.g^{-1}$, V is the volume of metal containing solution in contact with the sorbent in ml, C_i and C_e are the initial and equilibrium concentration of metal in the solution in mgl^{-1}, respectively and S is the amount of added NH_2-MCM-41 in g [20].

The Langmuir and Freundlich sorption isotherm models have been successfully applied to establish the relationship between the amount of Cd(II) adsorbed onto NH_2-MCM-41 and its equilibrium concentration in aqueous solution at 20, 30, 40 and 50 °C.

The most widely used isotherm equation for modeling of the adsorption data is the Langmuir equation that is written as follows [20]:

$$q_e = \frac{q_{max} b C_e}{1 + b C_e} \quad (3)$$

Where q_e is the amount of metal ion adsorbed in (mgg^{-1}), C_e is the equilibrium concentration of Cd(II) ions in mgl^{-1}, q_{max} *is* q_e for a complete monolayer in (mgg^{-1}) and b is the equilibrium constant that is referred to the bonding energy of sorption in mg^{-1}.

The Freundlich isotherm is an empirical equation that is based on the sorption of a sorbate on a heterogeneous surface of a sorbent, which is most commonly written as follows [20]:

$$q_e = K_f C_e^{1/n} \quad (4)$$

Where q_e is the amount of metal ion adsorbed in (mgg^{-1}), C_e is the equilibrium concentration of Cd(II) ions in mgl^{-1} and K_f (in mgl^{-1}) and $1/n$ are the Freundlich constants incorporating all factors affecting the adsorption process such as capacity and intensity.

The pseudo-first order and pseudo-second order models [21] were applied to describe the kinetics of adsorption. The pseudo-first- order rate equation is represented as:

$$\ln(q_e - q_t) = \ln q_e - K_1 t \quad (5)$$

Where q_t and q_e ($mg.g^{-1}$) are the amounts of Cd(II) ions adsorbed on to NH_2-MCM-41 at equilibrium and at time t (min), respectively, and K_1 (min^{-1}) is the pseudo-first order reaction rate equilibrium constant. The pseudo-first order considers the rate of occupation of sorption sites to be in proportion to the number of unoccupied sites. A straight line of $\ln(q_e - q_t)$ versus t (minute) indicates application of the pseudo-first order kinetics model. In a true pseudo-first order process, $-K_1$ and $\ln q_e$ parameters should be equal to the slope and intercept of plot of $\ln(q_e - q_t)$ against t, respectively. In many cases, the first order equation of Lagergren [22] does not fit well with the whole range of contact time and is generally applicable over the initial stage of the adsorption process [23].

Based on equilibrium adsorption, the pseudo-second order kinetic equation is expressed as:

$$\frac{t}{g_t} = \frac{1}{K_2 q_e^2} + \frac{t}{q_e} \quad (6)$$

Where, k_2 is the pseudo-second order rate constant in ($g.mg.^{-1}min^{-1}$). q_e and K_2 the parameters can be calculated by a curve-fitting program from the slope and intercept of $t.q_t^{-1}$ *(min.g.*mg^{-1}*)* versus t *(min)* plots, respectively. The thermodynamic parameters can be determined using the distribution coefficient (K) that is dependent on temperature. The change in free energy (ΔG^o), enthalpy (ΔH^o) and entropy (ΔS^o) associated with the adsorption process were calculated using following equation [24]:

$$\ln K = \frac{\Delta S^\circ}{R} - \frac{\Delta H^\circ}{RT} \quad (7)$$

Where, R is the universal gas constant (8.314 J/mol.K) and T is the temperature in K. According to Equation 7, ΔH^0 and ΔS^0 the parameters can be calculated by a curve- fitting program from the slope and intercept of $\ln K$ versus $1/T$ plots, respectively.

The distribution coefficient (K) is calculated from the concentration of Cd(II) in the initial concentration (C_i) and that of Cd(II) in the supernatant (C_e) after filtration according to the following equation [25]:

$$K = \frac{C_i - C_e}{C_e} \cdot \frac{V}{m} \quad (8)$$

Where V is the volume of the solution (ml), and m is the mass of the sorbent (g). The Gibbs free energy, ΔG^0, of specific adsorption was calculated from the well-known equation:

$$\Delta G° = \Delta H^o - T\Delta S° \quad (9)$$

2. 6. Column Adsorption Experimental Details Column operations are essential for industrial scale designing of the fixed-bed system. Solution containing the Cd(II) metal ions was pumped in an up-flow mode from a container to the bottom of the glass column with 6 mm internal diameter and 30 cm column length. The solution flow rate was monitored using a peristaltic pump (pump drive 5101, Heidolph, Germany). The objective of the column experiments was to study the effect of process parameters such as various bed heights (2, 4 and 6 cm) of NH_2-MCM-41, various inlet flow rates (0.4, 0.6, 1 $ml.min^{-1}$) and initial Cd(II) ions concentration (50, 100, 150 mgl^{-1}). After each experiment, the optimum condition was chosen for continuing the adsorption procedure. Effluent samples are collected after a regular interval and all the sorption experiments were carried out at the room temperature of 20 °C and initial pH of 5. The residual concentration of Cd(II) metal ions in aqueous sample was determined using atomic adsorption spectrophotometer as before.

2. 7. Continuous Data Analysis and Modeling The breakthrough curves showed the performance of fixed-bed column. The time for breakthrough appearance, and the shape of the breakthrough curve are very important characteristics for determining the operation and dynamic response of a sorption column [26]. The effluent concentration (C_t) from the column that reaches about 0.1% of the influent concentration (C_0) is the breakthrough time, t_b. The time where the effluent concentration reaches 95% is usually called the "point of column exhaustion", t_e [27]. The breakthrough curve is usually expressed by C_t/C_0 as a function of time or volume of the effluent for a given bed depth. The upper area in the breakthrough curve represents the amount of metal retained in the column (q_{total}, mg) that can be calculated from Equation (10)

$$q_{total} = \frac{Q}{1000} \int_{t0}^{t_{total}} (1 - \frac{C_t}{C_0})\, dt \quad (10)$$

Where Q is the flow rate ($ml.min^{-1}$) that can be calculated through dividing the effluent volume (V_{eff}, ml) by the total time (t_{total}, min)

$$Q = \frac{V_{eff}}{t_{total}} \quad (11)$$

The total amount of metal ions sent to the column (mg) can be calculated from the following expression,

$$m_{total} = \frac{C_0 \times Q \times t_e}{1000} \quad (12)$$

The total metal removal percentage ($R\%$) with respect to flow volume can be calculated from the ratio of metal mass adsorbed (m_{total}) to the total amount of metal ions sent to the column (q_{total}), given by Equation (13)

$$R\% = \frac{q_{total}}{m_{total}} \times 100 \quad (13)$$

The equilibrium adsorption capacity, q_e ($mg.g^{-1}$), and the equilibrium metal concentration, C_e ($mg.l^{-1}$) can be calculated using the following equations, respectively:

$$q_e = \frac{q_{total}}{m} \quad (14)$$

$$C_e = \frac{m_{total} - q_{total}}{V_{eff}} \times 100 \quad (15)$$

where, m is the mass of the adsorbent (g).

The mass transfer zone (MTZ) is the region of the bed where most of the adsorption occurs and moves up the bed column. MTZ can be calculated from the difference between column exhaustion time (t_e) and column breakthrough time (t_b) by the following expression:

$$MTZ = L\frac{t_e - t_b}{t_e} \quad (16)$$

Where, L is the bed height in cm.

Design of an adsorption column requires prediction of the concentration-time profile from breakthrough curve for the effluent discharged from the column. Several models were applied to predict the breakthrough curve and also to calculate the column kinetic constants and the maximum adsorption capacity of a column. The analysis of the breakthrough curve in this study was done using two models, namely, Thomas model [28] and the bed depth service time (BDST) model [29] which is a modified form of Bohart-Adams model. It is generally accepted that BDST offers the simplest approach and rapid prediction of adsorber design and performance [30]. BDST model was derived based on the assumption that forces like intra-particular diffusion and external mass transfer resistance are negligible and that the adsorption kinetics is controlled by surface chemical reaction between the solute in the solution and the unused adsorbent. This model also serves as a useful tool for comparing the performance of columns operating under different process variables. The BDST model was described by Equations (17):

$$t = \left(\frac{N_0}{C_0 u} H\right) - \left(\frac{1}{k C_0}\right) ln\left[\frac{C_0}{C_t} - 1\right] \quad (17)$$

where C_0 and C_t are inlet and effluent adsorbate concentration, respectively, K is the adsorption rate constant (mg.min^{-1}), N_0 is the sorption capacity of bed (mg.g^{-1}), H is the bed height (cm), t is the fix-bed adsorber service time to breakthrough (min) and u is the linear volumetric flow rate (cm.min^{-1}). A plot of service time t against H should generate a straight line, and hence it can be written as:

$$t = aH - b \quad (18)$$

Where a is the slope and b is the ordinate intercept. With slope equal to (N_0/C_0u) and intercept of $(-(1/kC_0)\ln((C_0/C_t)-1))$. From the slope and intercept, both N_0 and k are calculated.

Thomas model is one of the most general and widely used models in the column performance theory. Thomas or reaction model is based on the assumption that the process follows Langmuir kinetics of adsorption–desorption with no axial dispersion. Further, it is derived with the assumption that the rate driving force obeys 2nd order reversible reaction kinetics. Thomas model also assumes a constant separation factor but is applicable to either favorable or unfavorable isotherm. The Thomas model presented as Equations (19):

$$\frac{C_t}{C_0} = \frac{1}{1+\exp\left(\frac{k_{Th} q_{Th} m}{Q}\right) - K_{Th} C_0 V_{eff}} \quad (19)$$

where C_0 and C_t are the inlet and effluent adsorbate concentrations, respectively, k_{Th} (ml.mg^{-1}.min^{-1}) is the Thomas rate constant, q_{Th} (mg.g^{-1}) is the maximum adsorption capacity estimated by the Thomas model (mg.g^{-1}), m is the amount of adsorbent in the column, V_{eff} is the effluent volume (ml), and Q the flow rate (ml.min^{-1}). The Thomas model constants (k_{Th}, q_{Th}) can be determined from the plot of C_t/C_0 against time (min).

2. 8. Column Desorption and Regeneration Experiments After saturation with Cd(II) ions, the adsorbent material in the column was regenerated using 0.3M HCl solution at a flow rate of 0.8 ml.min^{-1} [14]. The concentration of Cd(II) in the regenerated solution was determined at different interval. To verify the performance stability of the activated sorbent column, three cycles of adsorption-regeneration process were performed. In each cycle, the regenerating agent was 0.3M HCl and the regeneration conditions were similar. After regeneration, the activated sorbent was washed with distilled water for 1 h and reused in the next cycle of the adsorption experiments. The uptake reduction percentage (*%E*) can be calculated by Equation (20)

$$\%E = \frac{q_1 - q_n}{q_1} \times 100 \quad (20)$$

Where, q_1 and q_n are metal uptake (mg.g^{-1}) at first stage and next stages (second and third stages), respectively.

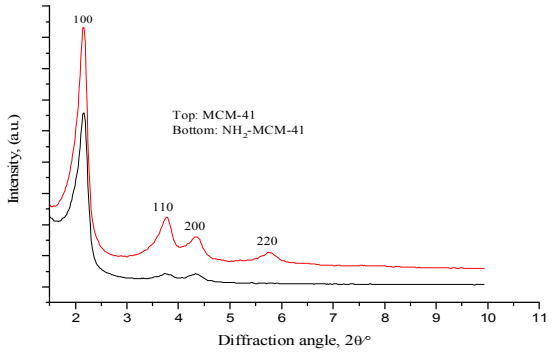

Figure 1. Low-angle XRD paterns of calcined MCM-41 and NH_2-MCM-41.

TABLE 1. Textural properties of calcined and functionalized MCM-41

Sample	S_{BET} (m^2/g)	D_{BJH} (nm)	V_{total} (cm^3/g)
MCM-41	1174	4.1	0.98
NH_2-MCM-41	787.97	3.3	0.81

3. RESULTS AND DISCUSSION

3. 1. Adsorbent Characterization The XRD pattern of MCM-41 and NH_2-MCM-41 are shown in Figure 1. These spectra indicate that one-dimensional hexagonal mesoporous structure of MCM-41was obtained. In the MCM-41 pattern we can see a very sharp (1 0 0) diffraction peak at 2.18 and three additional high order peaks (1 1 0, 2 0 0 and 2 1 0) with lower intensities at 3.78, 4.33 and 5.76, respectively[2].

d-spacing values for these XRD peaks were 40.52, 23.35, 20.37 and 15.31 ˚A, respectively. A unit cell parameter, a_0, of 46.79 ˚A was obtained using the following equation [31]:

$$a_0 = \frac{2d_{100}}{\sqrt{3}} \quad (21)$$

For NH_2-MCM-41, a considerable decrease in the XRD peaks intensity was observed. It should be noted that the intensity decrease in the (1 0 0) peak for functionalized MCM-41 providing further evidence of functionalization occurring mainly inside the mesopore channels. Collectively, the XRD pattern of the functionalized MCM-41 also suggest not only a significant degree of short range ordering of the structure and well-formed hexagonal pore arrays of the samples, but also the maintenance of the structural order of the synthesized materials after functionalization. Physical parameters of nitrogen isotherms containing the Barret-Joyner-Halenda average pore diameter (D_{BJH}), the Brunauer-Emmett-Teller surface area (S_{BET}) and the total pore volumes (V_{total}) of the calcined MCM-41 and the NH_2-MCM-41 samples are summarized in Table 1.

After functionalization, a decrease in the S_{BET} and D_{BJH} average pore diameter was observed that can be easily interpreted due to the fact that the presence of pendant group on the surface that partially blocks the adsorption of nitrogen molecules.

The wall thickness of MCM-41 was 5.79 ˚A where calculated by the following equation [31]:

$$\text{wall thickness} = \frac{2d100}{\sqrt{3}} - D_{BJH} \quad (22)$$

The adsorption and desorption isotherms of nitrogen on each sample show the typical type IV isotherm according to the IUPAC nomenclature for parent MCM-41 and NH_2-MCM-41 (see Figure 2).

FTIR spectroscopy was used to detect the presence of organic groups in the calcined MCM-41 and amino functionalized MCM-41 (see Figure 3).

The vibration signals around 1100, 793 and 457 cm^{-1} present in both samples are typical Si-O-Si bands attributed to the asymmetric stretching, symmetric stretching and bending, respectively [14, 32]. The absorption band for H-O-H bending vibration in water is at around 1650 cm^{-1}. The spectra showed a broad band around 3070–3750 cm^{-1}, which is due to adsorbed water molecules. Presence of the peak around 1550 cm^{-1} is mainly from the NH_2 symmetric bending vibration, absent in neat MCM-41, indicates the successful grafting of organic amine onto the surface [11, 33]. Also, in the NH_2-MCM-41 spectra the absorbance peaks appear in 2916 and 2846 cm^{-1} that corresponding to asymmetric and symmetric C-H stretching in the propyl chain [34]. The absorbance of the C-N stretching vibration is normally observed around 1000-1300 cm^{-1}[35]. However this peak cannot be resolved due to its overlap with the absorbance of Si–O–Si stretch in the 970-1350 cm^{-1}.

The thermograms of the sorbents are presented in Figure 4. The TGA curve of the uncalcined MCM-41 shows four steps of weight loss (30-150 °C, 150-300 °C, 300 °C-600 °C and >600 °C).

The weight loss is 6.27% in the first step and is associated with desorption of water. The weight losses in the second and third steps (37.43%) are mainly associated with oxidative decomposition of organic surfactant inside the pores. In the final step, the weight loss (1.05%) is mainly due to water loss formed by the condensation of silanol groups. The thermogram of the calcined MCM-41 shows two steps of weight loss. The weight loss is 9.23% in the first step from 30 °C to 110 °C that is associated with desorption of water and in the second step (110-840 °C), the weight loss (2.81%) is mainly due to water loss formed by the condensation of silanol groups. The thermogram of the amino-functionalized MCM-41 shows a gradual weight loss up to 840 °C. The TGA curve of the NH_2-MCM-41 shows four steps of weight loss (30-130 °C, 130-340 °C, 340 °C-600 °C and >600 °C). The weight loss is 7.59% in the first step and is due to desorption of physisorbed water held in the pores. The weight losses in the second and third steps (11.23%) are mainly associated with oxidative decomposition of organic functional groups.

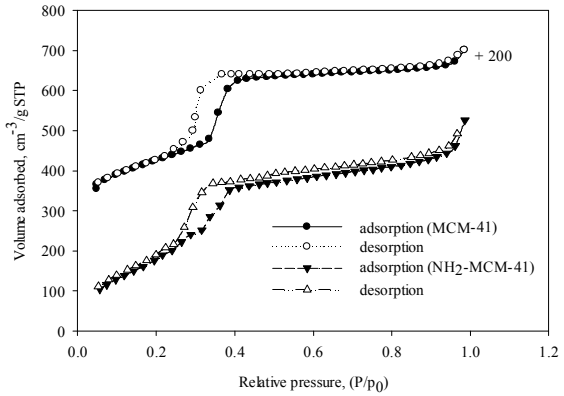

Figure 2. Nitrogen adsorption-desorption of parent MCM-41 and NH_2-MCM-41

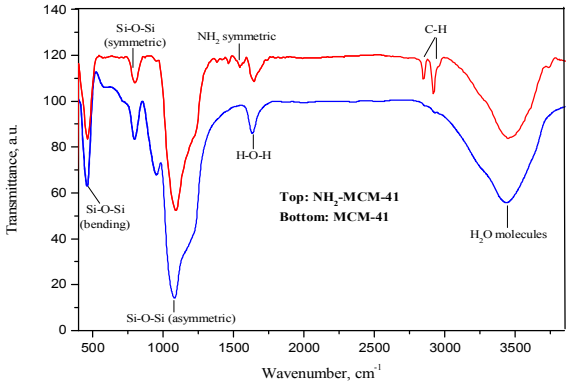

Figure 3. FT-IR spectra of MCM-41 and NH_2-MCM-41

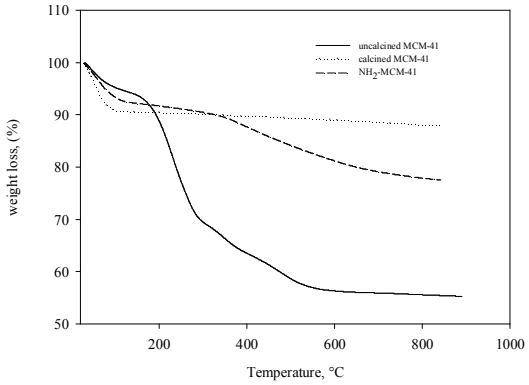

Figure 4. Thermograms of the uncalcined MCM-41, calcined MCM-41 and NH_2-MCM-41.

In the final step, the weight loss (3.67%) is due to the dehydroxylation of the silicate networks. On the basis of elemental analysis, the amount of functional groups was calculated to be 0.675 mmol.g^{-1}of MCM-41.

3. 2. Adsorption Study in Batch System

3. 2. 1. Effect of Sorbent Dosage In order to establish appropriate adsorbent type and dose for Cd(II) ions removal the experiments with different dosage of MCM-41 and NH_2-MCM-41 were performed. The Figure 5 shows the results of removal efficiency and metal uptake of Cd(II) ions. Observed that in MCM-41, the percentage removal increased and metal uptake decreased with the increasing of the adsorbent dosage. The maximum removal efficiency was 42% at a sorbent dose of 2 g.l^{-1} and maximum metal uptake was 21.46 mg.g^{-1} at a sorbent dose of 1.5 g.l^{-1}. However, NH_2-MCM-41 shows much larger Cd(II) removal efficiency compared to MCM-41. As shown in Figure 5 the removal efficiency of Cd(II) from aqueous solution increased significantly from 10.85% to 100% when the adsorbent dosage of NH_2-MCM-41 increased from 0.1 to 3.5 gl^{-1}.

This might be due to the grafted amine groups on the pores of mesoporous silica and its more active adsorption sites [12]. The results also revealed that the maximum metal uptake by NH_2-MCM-41 was 112 mg.g^{-1} at a sorbent dose of 0.1 g.l^{-1} and metal uptake decreased with increasing of the adsorbent dosage. It has been reported by previous study [11] that MCM-41 chemically modified by an amine group showed maximal removal efficiency of 93% for Cd(II) at a dose of 5 g.l^{-1}.

3. 2. 2. Effect of pH Solution on Adsorption The effect of initial pH on the adsorption process in the range of 2-8 is presented in Figure 6. The pH of the solution is an important factor in the adsorption process, which affects surface charge of the adsorbent and the degree of ionization and speciation of adsorbate.

As seen in Figure 6, the removal efficiency of Cd(II) increased with increasing of solution pH from 2 until it reaches a maximum at 5, and decreases at the pH value higher than 5. The removal efficiency was 7.24% at pH 2 and these values increased to 77.07% with pH increasing to 5. The increase in metal ion removal as pH increases can be explained on the basis of a decrease in H^+ on the surface sites and by a decrease in positive surface charge, which results in less repulsion of adsorbing metal ions. Lower uptake at lower pH values was due to the protonation of the amine moieties [36]. However, on increasing the pH further, the metal speciations in solution may become an important factor and the increase in Cd(II) removal has been attributed to reduced solubility and tend to precipitate out of solution in the hydroxide form [14].

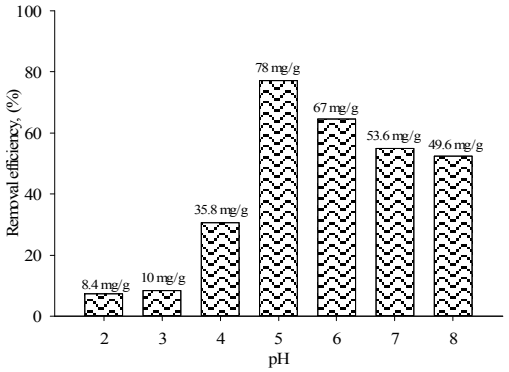

Figure 6. Effect of pH level on adsorption at 100 mgl^{-1} of Cd(II) concentration and a sorbent dose of 1 gl^{-1}

.

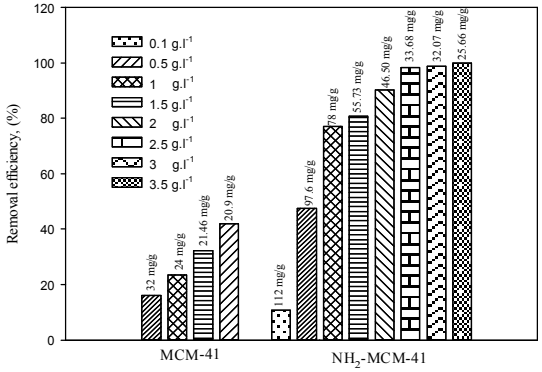

Figure 5. Effect of sorbent type and dose on metal ion adsorption at 100 mgl^{-1} of Cd(II) concentration and pH level of 5.

TABLE 2. Constants of Langmuir and Freundlich isotherms for Cd(II) ions adsorption by NH_2-MCM-41.

Langmuir			Freundlich		
B	q_{max}	R^2	n	K_f	R^2
1.68	90.92	0.98	6.19	46.70	0.92

3. 2.3. Adsorption Isotherms

The Langmuir and Freundlich constants and their correlation coefficients (R^2) evaluated from two isotherms from the nonlinear Langmuir and Freundlich plots by plotting q_e versus C_e (Figure 7) are given in Table 2.

The sorption characteristics of Cd(II) on the NH_2-MCM-41 followed more closely the Langmuir isotherm model than the Freundlich isotherm model that may be due to the homogenous distribution of active sites on the NH_2-MCM-41 surface, since the Langmuir equation assumes that the surface is homogenous and all sites have equal adsorption energies [11]. Both isotherms showed a sharp initial slope indicating that the

adsorbent operates at high efficiency at a low metal concentration and gets saturated with an increased ions concentration. This observation is further supported by evaluation of the respective correlation coefficients [37], which is a measure of how well the predicted values from a forecast model match the data from the experiment (Table.2). The main reason for this trend is the electrostatic interaction between adsorbent molecules and the adsorbate. There is also hydrophobic interaction between the amino groups and heavy metal ions [38].

Maximum adsorption capacity, q_{max}, for complete monolayer coverage is 90.92 $mg.g^{-1}$. Comparison of q_{max} of present study with previous works revealed that adsorption capacity of NH_2-MCM-41 is very high [2, 11, 14]. On the other hand, the value of *n*, indicative of high adsorption intensity under studied conditions.

3. 2. 4. Adsorption Kinetics In the present study, the two kinetic models mentioned above (5-6) were used to describe Cd(II) ion adsorption by NH_2-MCM-41. The degree of conformity between data from the experiment and values of the predicted model was expressed by the coefficient of determination (R^2). A relatively high R^2 value for the relationship between measured and predicted Cd(II) adsorption data indicated that the model successfully described kinetic activity. It should be noted that a high R^2 for a particular kinetic model does not necessarily mean that this equation is the best. The results of the kinetics parameters for Cd(II) ions, calculated from the linear plots of pseudo-first order and pseudo-second order kinetics models are presented in Table 3.

The low correlation coefficient values obtained for the pseudo-first order model indicates that sorption of metal ions did not follow the pseudo-first order reaction (Figure not shown). Most of the calculated values of q_{e1} from the first-order kinetics model are lower than those from the experiment ($q_e^{exp.}$). The insufficiency of the pseudo-first order model to fit the kinetics data could possibly be due to limitations of the boundary layer that controls the sorption process.

It was observed that data from the experiment fitted well to the pseudo-second order equation than pseudo-first order (Figure 8), which is based on the sorption capacity of the solid phase. The correlation coefficients (R^2) for the linear plots of t/q_t against *t* for the pseudo-second order equation were observed to be close to 1 for Cd(II) ions. The theoretical *q*e (q_{e2}) values for metal ions were also very close to the values deduced from the experiment ($q_e^{exp.}$). These observations suggest that metal sorption by NH_2-MCM-41 followed the second-order reaction, suggesting that the process controlling the rate may be a chemical sorption involving valence forces through sharing or exchanging of electrons between sorbent and sorbate [39].

TABLE 3. Kinetic parameters for adsorption rate expressions

C_i (mgl^{-1})	$q_e^{exp.}$ (mgg^{-1})	Pseudo-first-order			Pseudo-second-order		
		q_{e1} (mgg^{-1})	K_1 (min^{-1})	R^2	q_{e2} (mgg^{-1})	K_2 (min^{-1})	R^2
10	10.0	6.19	0.031	0.560	9.89	2.944	0.9850
25	24.0	21.62	0.030	0.903	26.74	1.636	0.9970
50	49.3	53.15	0.039	0.924	58.82	0.873	0.9760
100	84.2	89.63	0.039	0.963	94.34	0.468	0.9640
150	91.2	73.96	0.047	0.996	102.04	0.402	0.8848
200	92.4	78.14	0.044	0.956	105.26	0.407	0.9653

C_i: initial Cd(II) concentration; $q_e^{exp.}$: experimental value; q_e1 and q_e2: calculated values; K_1, K_2 and K_i: rate constants.

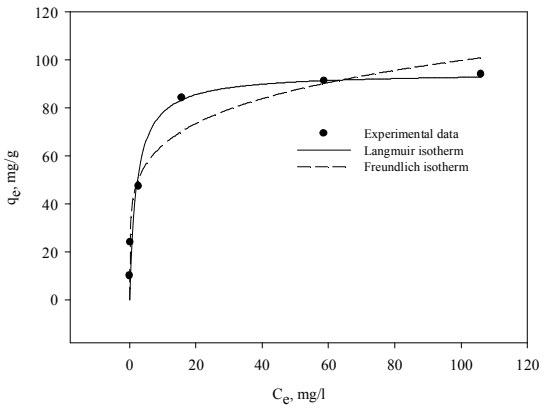

Figure 7. Langmuir and Freundlich isotherms for adsorption of Cd(II) ions on NH_2-MCM-41 with a sorbent dose of 1 $g.l^{-1}$ and pH level of 5

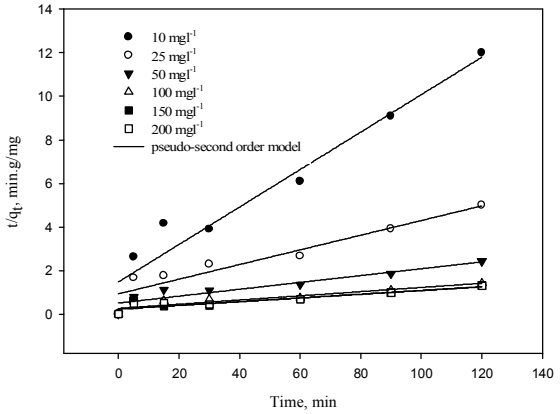

Figure 8. pseudo-second order equations for Cd(II) adsorption at 1 gl^{-1} of sorbent, pH level of 5 and various initial Cd(II) ion concentration.

3. 2. 5. Thermodynamic Studies The adsorption of Cd(II) ions increase with an increase of temperature and the value of ΔH^0 is positive, as shown in Figure 9. and the relative parameters and correlation coefficient calculated from Equations (7-9) are listed in Table 4.

The positive values of ΔH^o indicate the endothermic behavior of the adsorption reaction of Cd(II) ions and suggest that a large amount of heat is consumed to transfer the Cd(II) ions from an aqueous to a solid phase (NH_2-MCM-41). The ΔG^o for the adsorption process was as -39.51, -40.88, -42.23 and -43.58 kJ/mol at 293, 303, 313 and 323 K, respectively. The negative ΔG^o values at different temperatures were due to the fact that the adsorption process is feasible and thermodynamically spontaneous.

The value of ΔG^o that decreased with an increase in temperature indicated more efficient adsorption of Cd(II) at higher temperature. At higher temperature, ions are readily desolvated, and therefore their adsorption becomes more favorable. Generally, the change in free energy for physisorption is between -20 and 0 kJ mol^{-1}, but chemisorption is in the range of -80 to -400 kJ mol^{-1} [40]. The values of ΔG^o obtained in this study were within between these two ranges, indicating that the other adsorptions mechanism such as ion exchange and surface complexation are likely the dominating mechanisms. The positive values of entropy change (ΔS^o) reflect the affinity of adsorbent material (NH_2-MCM-41) to Cd(II) ions in aqueous solutions and suggest that some structure change has taken place in the adsorbent.

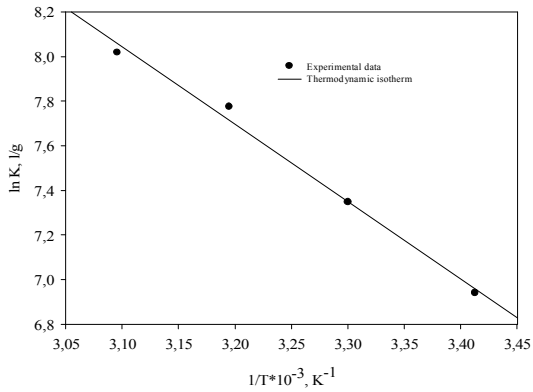

Figure 9. Plots of (a): C_e versus time and (b): ln k versus $1/T*10^{-3}$, for Cd(II) adsorption on NH_2-MCM-41 at a sorbent dose of 1 gl^{-1}, pH 5.0, 150 mgl^{-1} of Cd(II) concentration and different temperatures

3. 3. Column Results

3. 3. 1. Effect of Different Bed Height on Breakthrough Curve The breakthrough curves at three different bed heights of 2, 4, and 6 cm (0.414, 1.056 and 1.5 g) at a constant flow rate of 0.4 $ml.min^{-1}$ and influent concentration of 100 $mg.l^{-1}$ of Cd(II) are presented in Figure 10 and the breakthrough analysis summarized in Table 5.

It is clear that as the bed height increased both the breakthrough and the exhaust times increased due to the more contact time. The experimental breakthrough times (corresponding to effluent concentration 0.1 $mg.l^{-1}$), for bed heights of 2, 4, and 6 cm were found to be 30, 83 and 143 minutes, respectively (see Table 5).

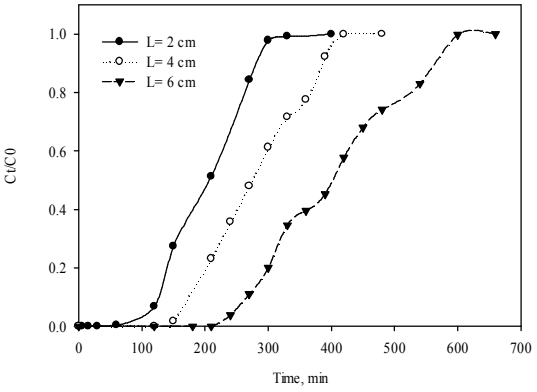

Figure 10. Effect of various beds high on the breakthrough curve of Cd(II) adsorption on NH_2-MCM41: initial Cd(II) concentration 100 $mg.l^{-1}$; flow rate 0.4 $ml.min^{-1}$; pH 5.

TABLE 4. Thermodynamic parameters of Cd(II) adsorption on NH_2-MCM-41 at different temperatures in Kelvin (initial concentration of metal ions was 150 $mg.l^{-1}$)

ΔH°, J/mol	ΔS°, J/mol·K	-ΔG°, kJ/mol				R^2
		293°K	303°K	313°K	323 °K	
22.60	134.93	-39.51	-40.88	-42.23	-43.58	0.998

The slope of breakthrough curve decreased with increasing bed height, which resulted in a broadened mass transfer zone. So that, when the bed height increased, the MTZ length approximately increased from 1.79 to 3.15 and 4.49 cm, respectively. As shown in Table 5, the bed height influenced the Cd(II) uptake capacity (q_e) of 19.49, 10.53 and 10.74 $mg.g^{-1}$, which was recorded at 2, 4 and 6 cm, respectively. The increase in the metal uptake capacity with the increasing bed height in the fixed-bed column reported ***in the literatures*** [14, 41]. However, we expected that the metal adsorption per unit mass (qe) of NH_2-MCM-41 would be relatively decreased with the increasing bed height and the bed with 2 cm height showed the highest qe in comparison to the ones with 4 cm and 6 cm height, which this may be due to that high adsorbent mass (1.056 and 1.5 g) was too great to utilize all of the capacity for the given conditions (Q = 0.4 $ml.min^{-1}$ and C_0 = 100 $mg.l^{-1}$).

TABLE 5. The breakthrough parameters and Thomas model constants for Cd(II) removal at various column conditions.

Column conditions [a]			Breakthrough analysis [b]						Thomas model [c]		
L	**Q**	**Conc.**	t_b	t_e	C_e	q_e	**R%**	**MTZ**	q_{TH}	K_{TH}	R^2
2	0.4	100	30	290	2.20	19.49	69.57	1.79	19.52	0.016	0.995
4	0.4	100	83	395	2.44	10.53	70.36	3.15	10.49	0.012	0.991
6	0.4	100	143	570	2.53	10.74	70.69	4.49	10.62	0.009	0.988
4	0.4	100	83	395	2.37	10.65	71.23	3.15	10.54	0.012	0.986
4	0.8	100	47	295	2.14	16.60	72.75	3.36	16.43	0.018	0.996
4	1	100	30	225	3.09	15.40	62.38	3.53	15.36	0.017	0.996
4	0.8	50	81	530	1.13	14.53	74.29	3.38	29.14	0.011	0.993
4	0.8	100	47	295	2.14	16.59	72.75	3.36	16.43	0.018	0.996
4	0.8	150	4	170	4.31	11.38	59.37	3.92	7.54	0.029	0.997

[a] L: bed height (cm); Q: flow rate (ml.min^{-1}); Conc: influent metal ion concentration (mg.l^{-1}).
[b] t_b: column breakthrough time (min) t_e: column exhaustion time (min); C_e: equilibrium concentration (mg.l^{-1}); q_e: adsorption capacity (mg.g^{-1}); R%: removal percentage; MTZ: mass transfer zone (cm).
[c] k_{Th}: Thomas rate constant (ml.min^{-1}.mg^{-1}); q_{Th}: Thomas maximum adsorption capacity (mg.g^{-1}).
On the **other hand,** In a bed with a higher length a larger volume of the metal solution could be treated and a higher percent of metal removed, so that when the bed height increased (from 2 to 4 and 6) the removal efficiency (R %) increased from 69.57% to 70.36% and 70.69%, respectively; and also the equilibrium metal concentration (C_e) increased from 2.20 to 2.44 and 2.53 mg.l^{-1}, respectively. These results indicated that the bed high of 4 cm offered an optimum breakthrough curve. Therefore, the subsequent experiments were carried out with this bed high.

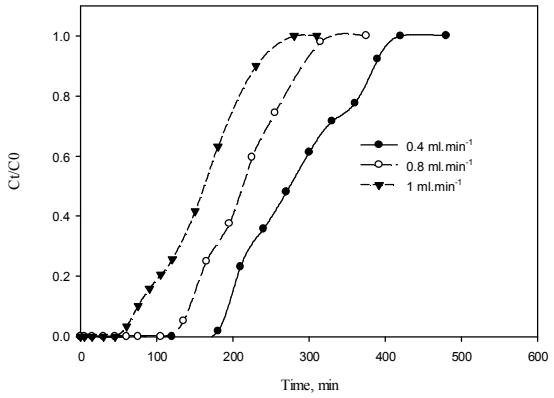

Figure 11. Effect of various flow rates on the breakthrough curve of Cd(II) adsorption on NH_2-MCM41: initial Cd(II) concentration 100 mg.l^{-1}; bed high 4 cm; pH 5.

3. 3. 2. Effect of Flow Rate In the second stage of removal studies in the fixed-bed column, the flow rate was changed (0.4, 0.8 and 1 ml.min^{-1}) while the inlet Cd(II) concentration in the feed was held constant at 100 mg.l^{-1} and the bed high was 4 cm (1.04 gr). The plots of effluent Cd(II) concentration versus time at different flow rates are shown in Figure 11 and the breakthrough parameters are presented in Table 5. These results reveal that as the flow rate increased, the breakthrough curve becomes steeper.

The breakthrough time and exhaustion time decreased and uptake capacity increased as the flow rate increased. The experimental breakthrough times, for flow rates 0.4, 0.8 and 1 ml.min^{-1} were found to be 83, 47 and 30 minutes, respectively. And also, the exhaust times were found to be 395, 295 and 225 minutes, respectively. The maximum bed capacities (q_e) were found as 10.65, 16.60 and 15.40 mg.g^{-1}, respectively. It was also found that the adsorbent gets saturated early at higher flow rate and the MTZ lengths for flow rates 0.4, 0.8 and 1 ml.min^{-1} were found to be approximately 3.15, 3.36 and 3.53 cm respectively. The reason for this behavior can be explained in the following ways: Firstly when the flow rate increased, the residence time of the solute in the column decreased, which causes the Cd(II) solution to leave the column before all the metal ions penetrate from the solution to the NH_2-MCM-41 pores and bind with amine functional groups [14, 42]. On the other hand, when the process is intra particle mass transfer controlled, a slower flow rate favors the sorption and when the process is subjected to external mass transfer control; a higher flow rate decreases the film resistance [43]. As revealed by Table 5, the removal efficiency (R%) of NH_2-MCM-4 remains relatively constant at a lower flow rates. when the flow rate increased from 0.4 to 0.8 ml.min^{-1} the removal efficiency increased by 1.52% but from 0.8 to 1 ml.min^{-1} the removal efficiency decreased by 10.37%; and also the equilibrium metal concentration (C_e) were 2.37, 2.14 and 3.09 mg.l^{-1}at flow rate 0.4, 0.8 and 1 ml.min^{-1}, respectively.

3. 3. 3. Effect of Influent Cd(II) Ions Concentration In the third stage of removal studies in the fixed-bed

column, The effect of the various influent Cd(II) ions concentrations (50 100 and 150 mg.l^{-1}) with the same adsorbent bed height (4 cm) and solution flow rate (0.8 ml.min^{-1}) were considered. The change in the initial metal ion concentration has a significant effect on breakthrough curve as illustrated in Figure 12. These results reveal that as the metal ions concentration increased, the breakthrough curve becomes steeper, also the breakthrough time, exhaustion time, and removal efficiency decreased as the concentration increased. These results demonstrate that the change of concentration gradient affects the saturation rate and breakthrough time, or in the other words, the volume of effluent treated per mass of a given adsorbent is a function of the influent concentration.

The experimental breakthrough times, for Cd(II) ions concentrations of 50 100 and 150 mg.l^{-1} were found to be 81, 7 and 4 minutes, respectively. And also, the exhaust times were found to be 530, 295 and 170 minutes, respectively. The maximum bed capacities (q_e) were found as 14.53, 16.59 and 11.38 mg.g^{-1}, respectively. It was also found that the adsorbent saturation is relatively same in different ions concentrations and the MTZ lengths for Cd(II) ions concentrations of 50 100 and 150 mg.l^{-1} were found to be approximately 3.38, 3.36 and 3.92 cm respectively.

3. 4. Breakthrough Curve Modeling Successful design of a column adsorption process requires prediction of the breakthrough curve for the effluent [44]. Over the years, several simple mathematical models have been developed for describing and analyzing the lab-scale column studies for the purpose of industrial applications [14, 30, 44]. So in this study, Thomas and BDST models were developed for predicting the dynamic behavior of the column.

3. 4. 1. Analysis of Cd (II) Ions Adsorption in Column by Thomas Model A non-linear regression analysis of Equation (19) was used to evaluate the Thomas model parameters of K_{Th} and q_{Th}. The comparison of the experimental and predicted breakthrough curves obtained at different bed height, flow rates and Cd(II) ions concentrations were evaluated by Thomas model (fitting curves are not shown).The calculated Thomas model parameters are listed in Table 5. The results indicated that they were all acceptable fits with coefficient correlation (R^2) ranging from 0.986 to 0.997. As can be seen from the results, the simulation whole breakthrough curve was well predicted by the Thomas model. As the bed height increase, the values of k_{TH} and q_{TH} decreased. The data in Table 5 also show a negligible difference between the experimental and predicted values of bed adsorption capacity. Also, as flow rate increased from 0.4 to 0.8 ml.min^{-1}, the values of k_{TH} and q_{TH} increased but by increasing flow rate from 0.8 to 1 ml.min^{-1} the values of k_{TH} and q_{TH} were encountered by small decreased. Also, by increasing the influent concentration, the values of k_{TH} considerably increased due to the driving force for adsorption. However, the decrease in the value of q_{Th} with increasing the influent concentration can be attributed to the high driving force for adsorption caused by the higher metal ions concentration [14].

3. 4. 2. Analysis of Cd(II) Ions Adsorption in Column by BDST Model The BDST model is based on physically measuring the capacity of the bed at different service time and bed height. The plot of service time (t_b) against bed height (Figure 13) was linear with high correlation coefficient (R^2=0.999) indicating the validity of the BDST model for the present system.

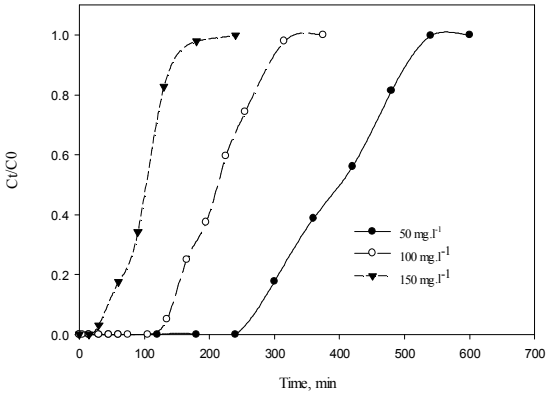

Figure 12. Effect of various influent Cd(II) ions concentration on the breakthrough curve of Cd(II) adsorption on NH_2-MCM41: solution flow rate of 0.8 ml.min^{-1}; bed high 4 cm; pH 5

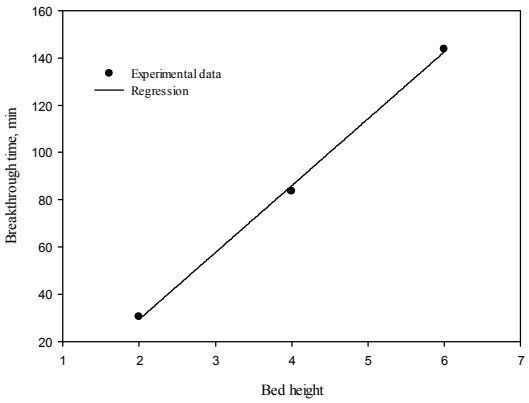

Figure 13. BDST model for Cd(II) sorption onto NH_2-MCM-41 in fixed bed column.

TABLE 6. BDST models constants for Cd(II) removal at various column conditions.

Column condition [a]			BDST model [b]			
Q	**Conc., mg/l**	**u**	**Equation**	**N_0**	**K**	**R^2**
0.4	100	1.41	t= 28.31H+27.33	3991	20.44	0.999

[a] Q: flow rate (ml.min^{-1}); Conc: influent metal ion concentration (mg.l^{-1}); u: linear volumetric flow rate (cm.min^{-1}) [b] N_0: sorption capacity of bed (mg.g^{-1}); K: adsorption rate constant (mg.min^{-1})

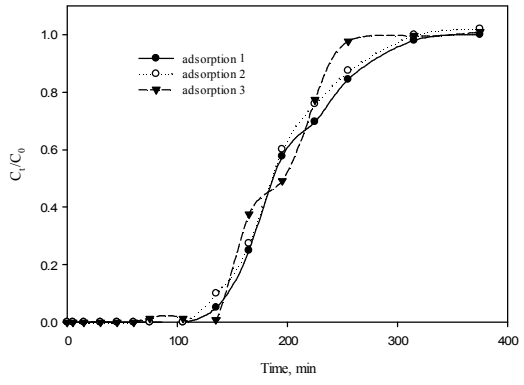

(a)

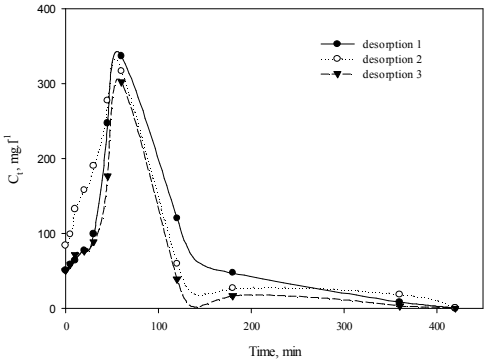

(b)

Figure 14. Column regeneration results: a) three cycles of breakthrough curve for Cd(II) adsorption, b) elution curves for three cycles of desorption.

The sorption capacity of bed per unit bed volume (N_0) and rate constant (k) was calculated from the slope and intercept of the BDST plot respectively and presented in Table 6.

The rate constant (*K*) characterizes the rate of solute transfer from the fluid phase to the solid phase. If *K* is large, even a short bed will avoid breakthrough, but as *K* decreases a progressively longer bed is required to avoid breakthrough [41]. Generally, the reported performance of NH_2-MCM-41 for cadmium ions removal in column is promising when compared to the other related studies [12, 41, 45]. The BDST model parameters can be useful to scale up the process for other flow rates without further experimental data and analysis.

3. 5. Column Desorption and Regeneration Results

Adsorption of Cd(II) on any sorbent can be by physical, chemical bonding, ion exchange or combination of all. If adsorption is by physical bonding then the loosely bound Cd(II) ions can be easily desorbed with distilled water. However, if the adsorption process is by chemical bonding or ion exchange or combination of both, then desorption can be affected by stronger elutes like acid or alkali solution. Thus, desorption and regeneration study can give a clear idea about the mechanism of adsorption along with the stability of the adsorbent for further use, which greatly reduces the process cost as well as the possibility of recovering the adsorbed metals. In this study, desorption were conducted with 0.3M HCl solution to desorption of Cd(II). After each elution operation, the de-ionized water was pumped through the column to eliminate the remaining acid in the bed, until a pH value between 4 and 5 was achieved in the effluent solution. Therefore, NH_2-MCM-41 was reused for three adsorption-desorption cycles at 4 cm bed height, 0.8 ml.min^{-1} flow rate and 100 mg.l^{-1} Cd(II) ion concentrations (Figure 14). It can be observed that the breakthrough curves in three cycles are relatively same (see Figure 14a). It means that the decrease in adsorption capacity of the adsorbent is not considerable in each cycle. The uptake reduction percentages according to Equation (20) were 3.28% and 4.75% for second and third cycles, respectively. From the experiments, it was observed that the elution curves of Cd(II) exhibited a high desorption rate in the first few minutes, the maximum concentration peak being achieved already in <60 minutes (see Figure 14b). The higher percentage of desorption indicated that ion exchange mechanism played significant role in the sorption process [45].

4. CONCLUSION

Based on the experimental study, the following results have been achieved out. It was concluded that pure and ordered MCM-41 materials could be successfully synthesized from silica powder that extracted from sedge. X-ray powder diffraction (XRD), BET and TGA and results of the parent mesoporous silica suggested their closeness of structural properties to those obtained from conventional silica sources. Also, characteristic evaluation revealed that obtained mesoporous materials defective sites (Si–OH) were successfully grafted with APTMS functional groups, which were then applied to adsorption of Cd(II) ions in both batch and fixed-bed column systems. The batch wise sorption experiments revealed that the maximum metal uptake by NH_2-MCM-41 was 112 mg.g^{-1} at a sorbent dose of 0.1 g.l^{-1}.

The optimum pH value for the removal of the Cd(II) ions from aqueous solution was pH 5. The isotherm study showed that the experimental data fitted well to the Langmuir model and the kinetics study revealed that data from the experiments fitted well to the pseudo-second order equation than pseudo-first order. The ion exchange and surface complication models controlled simultaneously during the adsorption process, and the surface complication model can be enhanced with increase of initial Cd(II) concentration and temperature. In continuous adsorption, the results obtained from the analysis of the breakthrough curves at various column conditions (bed height, flow rate, initial metal ion concentration) showed that the maximum sorption capacity of Cd(II) ions was obtained to be 19.49 $mg.g^{-1}$, at flow rate of 0.4 $ml.min^{-1}$ and bed height of 2 cm as the maximum *R*% was achieved 72.75%, at flow rate of 0.8 $ml.min^{-1}$ and bed height of 4 cm and 100 $mg.l^{-1}$ Cd(II) ions concentration. For the fixed-bed column system, the Thomas model was reasonably accurate in predicting the experimental column results for this study. The relationship between the bed depth and breakthrough time could be well fitted to the BDST model. The chemical stability of the NH_2-MCM-41 material allowed the reuse of the adsorbent material at least for three cycles in continuous mode. According to these observations NH_2-MCM-41 is a suitable sorbent for the removal of Cd(II) from water and wastewater in practical applications. Consequently, fundamentally the outlook is promising that the amine functionalized mesoporous silica MCM-41 has the potential of removing significant amounts of Cd(II) ions from aqueous solutions.

5. ACKNOWLEDGEMENT

The present research was sponsored by Tarbiat Modares University (TMU) and Iran Nanotechnology Initiative Council. We are grateful to Mineral Processing Engineering Department of Istanbul Technical University (ITU) for analytical and scientific supports.

6. REFERENCES

1. Sari, A. and Tuzen, M., "Biosorption of cadmium(ii) from aqueous solution by red algae (ceramium virgatum): Equilibrium, kinetic and thermodynamic studies", ***Journal of Hazardous Materials***, Vol. 157, (2008), 448-454.
2. Benhamou, A., Baudu, M., Derriche, Z. and Basly, J. P., "Aqueous heavy metals removal on amine-functionalized si-mcm-41 and si-mcm-48", ***Journal of Hazardous Materials***, Vol. 171, No. 1-3, (2009), 1001-1008.
3. Padma, V., Padmavathy, V. and Dhingra, S., C., "Kinetics of biosorption of cadmium on bakers yeast", ***Bioresour. Technol***, Vol. 89, (2003), 281-287.
4. Martínez, M., Miralles, N., Hidalgo, S., Fiol, N., Villaescusa, I., and Poch, J., "Removal of lead(ii) and cadmium(ii) from aqueous solutions using grape stalk waste", ***Journal of Hazardous Materials***, Vol. 133, No. 1-3, (2006), 203-211.
5. Unuabonah, E. I., Olu-Owolabi, B. I., Fasuyi, E. I. and Adebowale, K. O., "Modeling of fixed-bed column studies for the adsorption of cadmium onto novel polymer–clay composite adsorbent", ***Journal of Hazardous Materials***, Vol. 179, No. 1–3, (2010), 415-423.
6. Alvarez-Ayuso, E., Garcia-Sancheza, A. and Querol, X., "Purification of metal electroplating waste waters using zeolites", ***Water Research***, Vol. 37, (2003), 4855-4862.
7. Jiang, M.-q., Jin, X.-y., Lu, X.-Q. and Chen, Z.-l., "Adsorption of pb(ii), cd(ii), ni(ii) and cu(ii) onto natural kaolinite clay", ***Desalination***, Vol. 252, No. 1-3, (2010), 33-39.
8. Kadirvelu, K. and Namasivayam, C., "Activated carbon from coconut coirpith as metal adsorbent: Adsorption of cd(ii) from aqueous solution", ***Advances in Environmental Research***, Vol. 7, No. 2, (2003), 471-478.
9. Gao, Z., Wang, L., Qi, T., Chu, J. and Zhang, Y., "Synthesis, characterization, and cadmium(ii) uptake of iminodiacetic acid-modified mesoporous sba-15", ***Colloids and Surfaces A: Physicochemical and Engineering Aspects***, Vol. 304, No. 1–3, (2007), 77-81.
10. Abdollahi-Alibeik, M. and Pouriayevali, M., "Nanosized mcm-41 supported protic ionic liquid as an efficient novel catalytic system for friedlander synthesis of quinolines", ***Catalysis Communications***, Vol. 22, (2012), 13-18.
11. Heidari, A., Younesi, H. and Mehraban, Z., "Removal of ni(ii), cd(ii), and pb(ii) from a ternary aqueous solution by amino functionalized mesoporous and nano mesoporous silica", ***Chemical Engineering Journal***, Vol. 153, No. 1-3, (2009), 70-79.
12. Shahbazi, A., Younesi, H. and Badiei, A., "Batch and fixed-bed column adsorption of cu(ii), pb(ii) and cd(ii) from aqueous solution onto functionalised sba-15 mesoporous silica", ***The Canadian Journal of Chemical Engineering***, (2012).
13. Sepehrian, H., Ahmadi, S. J., Waqif-Husain, S., Faghihian, H. and Alighanbari, H., "Adsorption studies of heavy metal ions on mesoporous aluminosilicate, novel cation exchanger", ***Journal of Hazardous Materials***, Vol. 176, No. 3, (2010), 252-256.
14. Shahbazi, A., Younesi, H. and Badiei, A., "Functionalized sba-15 mesoporous silica by melamine-based dendrimer amines for adsorptive characteristics of pb(ii), cu(ii) and cd(ii) heavy metal ions in batch and fixed bed column", ***Chemical Engineering Journal***, Vol. 168, No. 2, (2011), 505-518.
15. Wloch, J., Rozwadowski, M., Lezanska, M. and Erdmann, K., "Analysis of the pore structure of the mcm-41 materials", ***Appl. Surf. Sci.***, Vol. 191, (2002), 368-374.
16. Son, W., J. , Choi, J., S. and Ahn, W., S. , "Adsorptive removal of carbon dioxide using polyethyleneimine-loaded mesoporous silica materials", ***Microporous and Mesoporous Materials***, Vol. 113, No., (2008), 31-40.
17. Bhagiyalakshmi, M., Yun, L. J., Anuradha, R. and Jang, H. T., "Utilization of rice husk ash as silica source for the synthesis of mesoporous silicas and their application to CO_2 adsorption through tren/tepa grafting", ***Journal of Hazardous Materials***, Vol. 175, No. 1, (2010), 928-938.
18. Jang, H. T., Park, Y., Ko, Y. S., Lee, J. Y. and Margandan, B., "Highly siliceous mcm-48 from rice husk ash for CO_2 adsorption", ***International Journal of Greenhouse Gas Control***, Vol. 3, No. 5, (2009), 545-549.
19. Ghorbani, F., Younesi, H., Mehraban, Z., Sabri Çelik, M., Ghoreyshi, A. A., and Anbia, M., "Preparation and characterization of highly pure silica from sedge as agricultural waste and its utilization in the synthesis of mesoporous silica

mcm-41", ***Journal of the Taiwan Institute of Chemical Engineers***, under reweave manuscript, (2012).

20. Ghorbani, F., Younesi, H., Ghasempouri, S. M., Zinatizadeh, A. A., Amini, M., and Daneshi, A., "Application of response surface methodology for optimization of cadmium biosorption in an aqueous solution by *saccharomyces cerevisiae*", ***Chemical Engineering Journal***, Vol. 145, No. 2, (2008), 267-275.
21. Yang, X. and Al-Duri, B., "Kinetic modeling of liquid-phase adsorption of reactive dyes on activated carbon", ***Journal of Colloid and Interface Science***, Vol. 287, No. 1, (2005), 25-34.
22. Lagergren, S., "Zur theorie der sogenannten adsorption geliister stoffe, kungliga svenska vetenskapsakademiens", ***Handlingar***, Vol. 24, No. 4, (1898), l-39.
23. Ho, Y. S. and McKay, G., "The sorption of lead(ii) ions on peat", ***Water Research***, Vol. 33, No. 2, (1999), 578-584.
24. Chen, C. and Wang, X., "Adsorption of ni(ii) from aqueous solution using oxidized multiwall carbon nanotubes", ***Industrial and Engineering Chemistry Research***, Vol. 45, No. 26, (2006), 9144-9149.
25. Wang, X., Chen, C., Hu, W., Ding, A., Xu, D., and Zhou, X., "Sorption of 243am(iii) to multiwall carbon nanotubes", ***Environmental Science and Technology***, Vol. 39, No. 8, (2005), 2856-2860.
26. Ahmad, A. A. and Hameed, B. H., "Fixed-bed adsorption of reactive azo dye onto granular activated carbon prepared from waste", ***Journal of Hazardous Materials***, Vol. 175, No. 1–3, (2010), 298-303.
27. Kundu, S., Kavalakatt, S. S., Pal, A., Ghosh, S. K., Mandal, M., and Pal, T., "Removal of arsenic using hardened paste of portland cement: Batch adsorption and column study", ***Water Research***, Vol. 38, No. 17, (2004), 3780-3790.
28. Thomas, H. C., "Heterogeneous ion exchange in a flowing system", ***Journal of the American Chemical Society***, Vol. 66, No. 10, (1944), 1664-1666.
29. Bohart, G. S. and Adams, E. Q., "Some aspects of the behavior of charcoal with respect to chlorine.1", ***Journal of the American Chemical Society***, Vol. 42, No. 3, (1920), 523-544.
30. Al-Degs, Y. S., Khraisheh, M. A. M., Allen, S. J. and Ahmad, M. N., "Adsorption characteristics of reactive dyes in columns of activated carbon", ***Journal of Hazardous Materials***, Vol. 165, No. 1–3, (2009), 944-949.
31. Zhao, D., Huo, Q., Feng, J., Chmelka, B. F. and Stucky, G. D., "Nonionic triblock and star diblock copolymer and oligomeric surfactant syntheses of highly ordered, hydrothermally stable, mesoporous silica structures", ***Journal of the American Chemical Society***, Vol. 120, No. 24, (1998), 6024-6036.
32. Li, J., Miao, X., Hao, Y., Zhao, J., Sun, X., and Wang, L., "Synthesis, amino-functionalization of mesoporous silica and its adsorption of cr(vi)", ***Journal of Colloid and Interface Science***, Vol. 318, No. 2, (2008), 309-314.
33. Parida, K. M. and Rath, D., "Amine functionalized mcm-41: An active and reusable catalyst for knoevenagel condensation reaction", ***Journal of Molecular Catalysis A: Chemical***, Vol. 310, No. 1–2, (2009), 93-100.
34. Zhao, H., Hu, J., Wang, J., Zhou, L. and Liu, H., "Co2 capture by the amine-modified mesoporous materials", ***Acta Physico-Chimica Sinica***, Vol. 23, No. 6, (2007), 801-806.
35. Sepehrian, H., Ahmadi, S. J., Waqif-Husain, S., Zolfaghari-Daryani, A. R. and Azadmousavi, M., "Adsorption studies of radionuclides and toxic metal ions on a modified mesoporous lanthanum(iii) silicate", ***Chinese Journal of Chemistry***, Vol. 28, No. 4, (2009), 561-566.
36. Alothman, Z. A. and Apblett, A. W., "Metal ion adsorption using polyamine-functionalized mesoporous materials prepared from bromopropyl-functionalized mesoporous silica", ***Journal of Hazardous Materials***, Vol. 182, No. 1-3, (2010), 581-590.
37. Sharaf, M. A., Arida, H. A., Sayed, S. A., Younis, A. A. and Farag, A. B., "Separation and preconcentration of some heavy-metal ions using new chelating polymeric hydrogels", ***Journal of Applied Polymer Science***, Vol. 113, No. 2, (2009), 1335-1344.
38. Adamczyk, Z. and Warszynski, P., "Role of electrostatic interactions in particle adsorption", ***Advances in Colloid and Interface Science***, Vol. 63, (1996), 41-149.
39. Ho, Y. S. and McKay, G., "Sorption of dye from aqueous solution by peat", ***Chemical Engineering Journal***, Vol. 70, No. 2, (1998), 115-124.
40. Chen, H., Zhao, J., Dai, G., Wu, J. and Yan, H., "Adsorption characteristics of pb(ii) from aqueous solution onto a natural biosorbent, fallen cinnamomum camphora leaves", ***Desalination***, Vol. 262, No. 1-3, (2010), 174-182.
41. Vijayaraghavan, K., Jegan, J., Palanivelu, K. and Velan, M., "Removal of nickel(ii) ions from aqueous solution using crab shell particles in a packed bed up-flow column", ***Journal of Hazardous Materials***, Vol. 113, No. 1–3, (2004), 223-230.
42. Malkoc, E., Nuhoglu, Y. and Abali, Y., "Cr(vi) adsorption by waste acorn of quercus ithaburensis in fixed beds: Prediction of breakthrough curves", ***Chemical Engineering Journal***, Vol. 119, No. 1, (2006), 61-68.
43. Ko, D. C. K., Porter, J. F. and McKay, G., "Optimised correlations for the fixed-bed adsorption of metal ions on bone char", ***Chemical Engineering Science***, Vol. 55, No. 23, (2000), 5819-5829.
44. Han, R., Zou, L., Zhao, X., Xu, Y., Xu, F., Li, Y., and Wang, Y., "Characterization and properties of iron oxide-coated zeolite as adsorbent for removal of copper(ii) from solution in fixed bed column", ***Chemical Engineering Journal***, Vol. 149, No. 1–3, (2009), 123-131.
45. Baral, S. S., Das, N., Ramulu, T. S., Sahoo, S. K., Das, S. N., and G, R. C., "Removal of cr(vi) by thermally activated weed salvinia cucullata in a fixed-bed column", ***Journal of Hazardous Materials***, Vol. 161, (2009), 1427-1435.

Aqueous Cadmium Ions Removal by Adsorption on APTMS Grafted Mesoporous Silica MCM-41 in Batch and Fixed Bed Column Processes

F. Ghorbani[a], H. Younesi[a], Z. Mehraban[b], M. Sabri Celik[c], A. A. Ghoreyshi[d], M. Anbia[e]

[a] *Department of Environmental Science, Faculty of Natural Resources, Tarbiat Modares University, 64414-356 Noor, Iran.*
[b] *New Technologies Committee, Research Institution for Curriculum Development and Educational Innovations, 1584634818, Tehran, Iran.*
[c] *Mining Engineering Department, Mineral and Coal Processing Section, Istanbul Technical University, Ayazaga, 80626 Istanbul, Turkey.*
[d] *Biotechnology Research Lab., Faculty of Chemical Engineering, Noshirvani University, Babol, Iran.*
[e] *Research Laboratory of Nanoporous Materials, Faculty of Chemistry, Iran University of Science and Technology, Farjam Street, Narmak, 16846, Tehran Iran.*

P A P E R I N F O

Paper history:
Received 23 November 2012
Recivede in revised form 11 December 2012
Accepted 13 December 2012

Keywords:
Sedge (*Carex riparia*)
MCM-41
Batch Adsorption
Fixed-bed Column

چکیده

در این مطالعه میان‌حفره سیلیکاتی منظم با ساختار شش وجهی با استفاده از سیلیس استخراج شده از خاکستر گیاه جگن (*Carex riparia*)سنتز شد.سپس ماده میان‌حفره سنتز شده با استفاده از ۳-آمینوپروپیل تری متوکسی سیلان (APTMS) عامل‌دار شد و ویژگی‌های ساختاری آن با استفاده از آنالیزهای پراش پرتو ایکس (XRD)، جذب-واجذب گاز نیتروژن، آنالیز وزن سنجی حرارتی (TGA) و طیف سنجی مادون قرمز فوریر (FT-IR) مورد بررسی قرار گرفت. در ادامه مواد سنتز شده جهت جذب یون‌های Cd(II) از محلول‌های آبی در سیستم‌های ناپیوسته و پیوسته بکار رفت. در سیستم ناپیوسته جذب پارامترهای غلظت اولیه یون‌های فلزی، دوز جاذب، زمان تماس، pH و دما مورد ارزیابی قرار گرفت. نتایج تعادلی جذب با استفاده از ایزوترم‌های لانگمیر و فرندلیچ با رگرسیون غیر خطی مورد آنالیز قرار گرفت. نتایج مطالعه سینتیک نشان داد که داده‌های تجربی بدست آمده برازش بهتری با مدل سینتیکی شبه درجه دوم نسبت به شبه درجه اول دارد. مطالعات ترمودینامیک نیز نشان داد که فرآیند جذب کاملاً وابسته به دما می‌باشد و ظرفیت جذب با افزایش دمای سیستم افزایش یافت، که نشان دهنده گرماگیر بودن و همچنین خودبخودی بودن فرآیند جذب است. برای آزمایش‌های جذب پیوسته جاذب NH_2-MCM-41 مورد استفاده قرار گرفت و منحنی‌های رخنه در ارتفاع ستون‌های مختلف جاذب، شدت جریان‌های مختلف و غلظت اولیه یون‌های فلزی مورد بررسی قرار گرفت. مدل توماس و BDST برای تعیین ثابت-های سینتیکی و برای پیش‌بینی منحنی‌های رخنه مورد استفاده قرار گرفت.

.

doi: *10.5829/idosi.ije.2013.26.05b.03*